J Math Chem (2010) 48:530–557
DOI 10.1007/s10910-010-9689-z

ORIGINAL PAPER

A new simple numerical model based on experimental scorch curve data fitting for the interpretation of sulphur vulcanization

G. Milani · F. Milani

Received: 25 September 2009 / Accepted: 23 April 2010 / Published online: 13 May 2010

Abstract Sulphur was the first agent used to vulcanize commercial elastomers (e.g. natural rubber) and allows meaningful cost reductions during the industrial process (production cost ratio between peroxides and accelerated sulphur is around 5). Therefore, accelerated sulphur vulcanization is the most popular technique for the production of polydiene and EPDM elastomers items. At present, crosslinking mechanisms are not analytically known in detail, therefore reticulation kinetic has to be deduced from mechanical properties obtained during standardized tests, as for instance the oscillating disc rheometer. In the present paper, we propose a numerical model to fit experimental rheometer data based on a simple composite three functions curve, able to describe the increase of the viscosity at successive curing times at different controlled temperature to use during the production of thick items vulcanized with sulphur. It is believed that rheometer curve is able to give an indirect information on the rubber reticulation kinetic at different temperatures, to use in a successive step to establish simplified analytical kinetic formulas to adopt in the accelerated sulphur vulcanization of polydiene and EPDM elastomers. In the model, it is necessary to collect rheometer curves at different specimen temperatures, because vulcanization in industrial practice occurs at variable temperatures during curing, with considerable differences from the core to boundary of the item. Once that rheometer curves are suitably collected in a database, they are used to predict the optimal vulcanization of real items industrially produced. Finally, a so called alternating tangent approach (AT) is implemented to determine optimal input parameters (curing external temperature

G. Milani (✉)
Politecnico di Milano, Piazza Leonardo da Vinci 32, 20133 Milano, Italy
e-mail: gabriele.milani@polimi.it; milani@stru.polimi.it

F. Milani
Via J.F. Kennedy 2, 45030 Occhiobello, Rovigo, Italy
e-mail: federico-milani@libero.it

T_n and rubber exposition time t) to use in the production process. Output mechanical property (objective function) to optimize is represented by the average tensile strength of the item. A meaningful example of engineering interest, consisting of a thick 2D EPDM cylinder is illustrated to validate the model proposed.

Keywords Sulphur vulcanization · Optimization · Rheometer curves fitting · Fourier's heat transmission law · Finite element method (FEM)

1 Introduction

Sulphur vulcanization is the most practical method for bringing about the drastic property changes described by the term vulcanization, not only in natural rubber but also in the diene synthetic elastomers, such as SBR, butyl, nitrile and EPDM rubbers.

Since the chemical reactions associated with the vulcanization are varied and involve only a few atoms in each polymer molecule, a definition of vulcanization in terms of the physical properties of the rubber is necessary. In this sense, vulcanization may be defined as any treatment that decreases the flow of an elastomer, increases its tensile strength and modulus, but preserves its extensibility.

Elemental sulphur is the predominant vulcanizing agent for general-purpose rubbers. It is used in combination with one or more accelerators and an activator system comprising zinc oxide and a fatty acid (normally stearic acid). The most popular accelerators are delayed-action sulphenamides, thiazoles, thiuram sulphides, dithiocarbamates and guanidines, etc. Part or all of the sulphur may be replaced by a sulphur donor such as a thiuram disulphide.

Despite the great diffusion and popularity of such kind of vulcanization process, probably related to the fact that sulphur is the most common method to vulcanize natural rubber, all the dienic family rubbers and EPDM elastomers, its chemistry of vulcanization is somewhat complex and has not been well understood throughout the century of the practice of the process since its discovery by Goodyear in 1839 [1–3], see Fig. 1. In particular, because of the prohibitive complexity of the reactions induced by sulphur during crosslinking -differently to peroxidic curing- no precise reaction kinetic formulas are available in the technical literature.

In this context, the aim of the work hereafter presented is to propose a two-step combined experimental and numerical procedure for the interpretation of accelerated sulphur curing, aimed at the optimal vulcanization of thick rubber compounds.

The approach relies in the following two steps:

1. For a given rubber compound, rheometer curves are experimentally evaluated at different vulcanization temperatures, ranging from low to high. Rheometer curves are obtained thought the so-called oscillating disc rheometer, as described by the ASTM 2084-81 [4]. It consists in a small rubber specimen subjected to fixed and controlled external curing temperature and in an oscillating disk for which the resistance to rotation is monitored as output parameter. The output information provided experimentally by the rheometer is the oscillation resistance (measured in [dNm]) as a function of the curing time. Such curve is characteristic

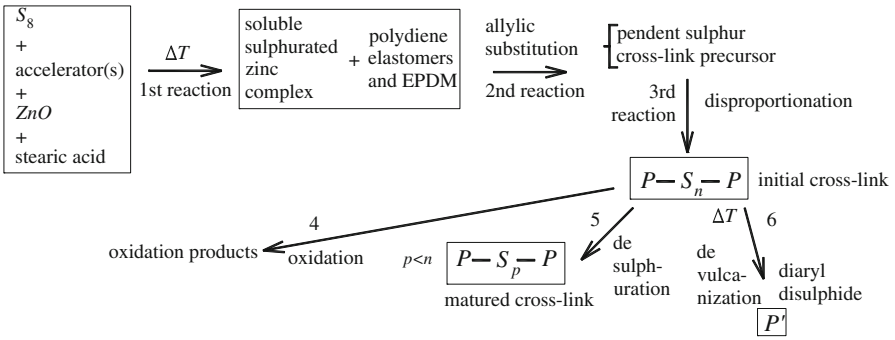

Fig. 1 Products and schematic reaction mechanisms of accelerated sulphur vulcanization of poly-diene and EPDM elastomers

of the rubber compound investigated and obviously changes varying the external curing temperature. In order to have a precise insight into the sulphur vulcanization kinetic, in absence of standard chemical reaction kinetics available, it is authors' opinion that the rheometer curve, repeated at different external curing temperatures, is the best way to have a quantitative information on the crosslinking density obtained at different temperatures and curing time for sulphur vulcanization, correlated between the network structure and elastic and dynamic properties of the item. The higher is the number of curves collected, the more precise is the database collected describing the curing behaviour at different temperatures of the compound analyzed.

2. The second step is to consider the industrial production process of real thick rubber items by means of the FE method. Such numerical approach provides the temperature profiles at increasing curing times for each point of the thick item. Obviously, each point undergoes different temperatures and such differences are more marked passing from the external layer to the core. By means of the database collected in the first step (rheometer curves), the corresponding crosslinking density level for each point of the item can be numerically evaluated [5,6], and hence output mechanical properties may be estimated.

From the above considerations, it is worth noting that the approach here proposed is somewhat different with respect to previously presented models suitable for the analysis of rubber cured with peroxides [7–13]. In this latter case, in fact, kinetic reaction equations are available and basically follow Arrhenius law [12,13]. For sulphur vulcanization, the reaction kinetic is much more intricate and requires an experimental characterization of the compound itself (first step).

In order to asses the capabilities of the two-step approach proposed, in the paper, an example of engineering interest is analyzed in detail, consisting of a rubber thick with cylindrical shape of external diameter approximately equal to 24 mm. The compound used to realize the cylinder is an EPDM rubber with a medium amount of propylene content (about 40% in weight) and 4.5% in weight on ENB, vulcanized through accelerated sulphur, as described in detail next.

A so called alternating tangent approach (AT) is implemented to determine optimal input parameters (curing external temperature T_n and rubber exposition time t) for the example at hand. Output mechanical property (objective function) to optimize is represented by the average tensile strength of the item.

Since the numerical model proposed requires an experimental validation to be completely predictive, a full experimental campaign is planned by the authors comprising both (a) the collection of a detailed database of scorching curves at different temperatures and varying compound typology and (b) the vulcanization of full scale industrial items varying both curing time and vulcanization external temperatures.

2 3D rubber thick elements vulcanization

At present, vulcanization of rubber thick elements with sulphur is a very difficult task, causing several technical problems to manufacturers. Usually, a theoretical approach is not taken into consideration, due to the complexity of the problem itself, with the subsequent adoption of empirical approaches. Unfortunately, sulphur vulcanization kinetics are not analytically known and no mathematical formulations commonly accepted are available in the literature, as it occurs for instance with peroxidic curing or silicon vulcanization [5–13]. Further problems are related to the impossibility to assure, during the vulcanization process, a homogeneous distribution of temperatures between internal (cool) zone and external (hot) boundaries. As a matter of fact, this always results in an over-vulcanization of the external coating and an insufficient curing of the internal regions of the elements. Consequently, resultant cured elements are almost always of poor quality and can not have a large widespread in engineering applications.

A great amount of the items available in the commercial market are obtained by extrusion, see Fig. 2. Manufacturing of rubber products always involves the following steps: mixing, shaping and vulcanization.

In the most common case of the industrial process of extrusion, we can schematically assume that a heating zone is followed by a cooling phase with water and/or air. In the first phase, cross-linking of polymer is obtained by curing with increasing temperature transmitted from the boundary to each point of the element by conduction or heat convection. Finally the resultant cured object is leaved and cooled in the surrounding air by free convection, Fig. 2. With the aim of optimizing the production line, many parameters have to be chosen carefully. In particular, the following variables play a crucial role: exposition time, temperature of the heating phase and temperature of the cooling phase.

3 Vulcanization process through sulphur: the oscillating disk cure meter

Vulcanization is the process where viscous and tacky rubber is converted into an elastic material through the connection of the long polymer chains with chemical bonds resulting in a 3D structure.

In the sulphur vulcanization, zinc oxide and fatty acid constitute the activator system, where the zinc ion is made soluble by salt formation between the acid and the oxide).

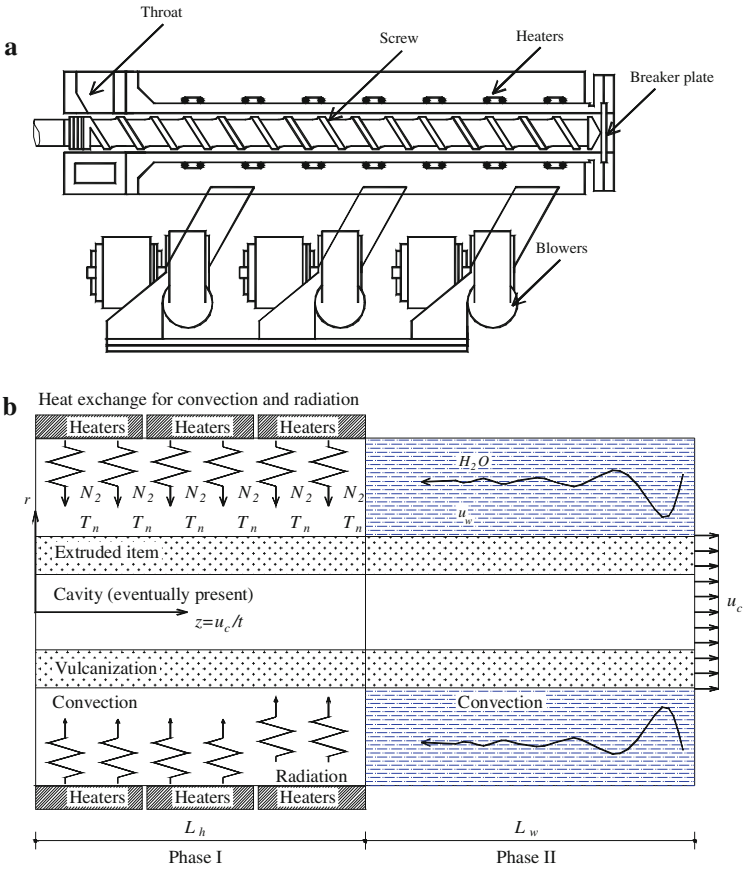

Fig. 2 Production of rubber items by extrusion. **a** Extrusion screw. **b** Schematic representation of the vulcanization phases (vulcanization: Phase I length L_h; cooling: Phase II length L_w)

Typical accelerators are MBT (2-mercaptobenzothiazole), MBTS (2,2'-dithiobisbenzothiazole), MTB (2-morpholinothio) benzothiazole, etc.

Different types of accelerators give vulcanization characteristics which differ in resistance to scorch (premature vulcanization) and the rate of vulcanization after cross-linking formation starts. In order to inhibit the premature vulcanization, some retarders are frequently used to control the scorch with little or no effect on the rate of cross-linking formation.

From the above considerations, it appears clear that to predict the vulcanization process is a very difficult task, the reaction process being a consequence of several concurring factors and depending on a number of input variables.

3.1 The cure meter vulcanization curve

The vulcanization characteristics of vulcanizable rubber compounds is experimentally determined by means of an oscillating disk cure meter (ASTM D 2084 [4]).

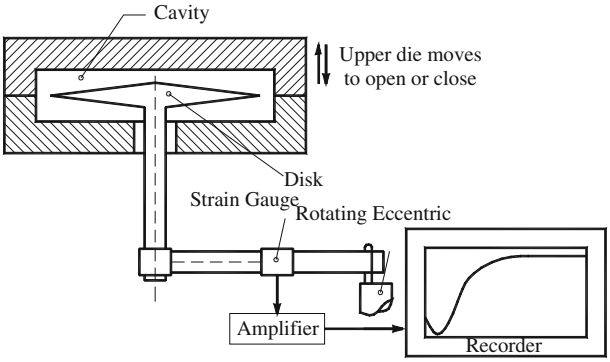

Fig. 3 Schematic representation of a rheometer for the determination of the curing kinetic of a rubber compound vulcanized with accelerated sulphur

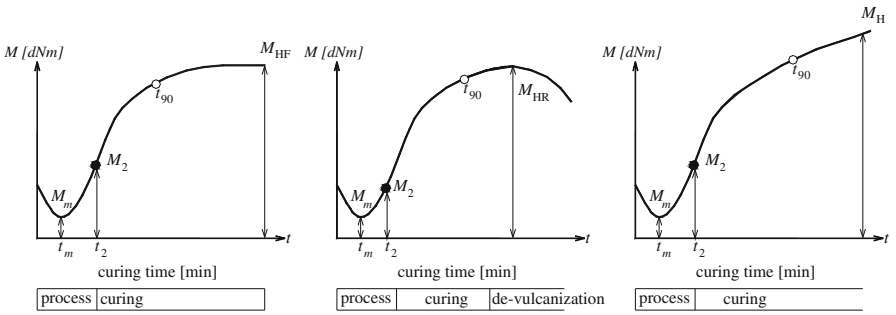

Fig. 4 Typical experimental behaviour of a rubber compound during rheometer test

The cure meter is a specialize laboratory device capable of measuring the extent of cure of a single sample at a given temperature on a continuous basis (see Fig. 3). The most popular of these instruments are of the oscillating disk variety [4]. The disk has a diameter of 20 mm and a thickness of 12.5 mm, so that the volume is 196.25 mm^3 and approximately 0.2 grams of compound are used. Since 0.2 grams of compound are used as specimen, it is pretty obvious that the temperature imposed to the rheometer remains essentially constant during all the laboratory test and therefore it is not influenced on the % of vulcanization that occurs before the test is started, at least on the range of temperatures of engineering interest, i.e. between 100 and 250 °C. The test sample of rubber is cured automatically in a cavity, while a disk embedded in the sample rotates in a oscillatory fashion through a small arch. The frequency of oscillation can be varied, as can the size of the arch. The resistance to oscillation is measured and recorded as a function of the time on a so-called rheometer chart like the one shown in Fig. 4. It is worth noting that, in the oscillation disk, the curing temperature has to remain constant during all the vulcanization process. Looking at the rheometer curve, three different cases can be encountered in practice, see Fig. 4: (a) the curve reaches a maximum asymptotically, (b) the curve reaches a maximum and then decreases and (c) the curve increases monotonically after the scorching time t_2.

Scorch time t_2 is defined as the time to incipient cure and mathematically represents the point at which second derivative of the rheometer curve is equal to zero. A torque equal to M_2 is reached at the scorching time. We define also t_{90} and t_{100} times in the rheometer curve: t_{90} time is approximately the time at which 90% of cross-linking is occurred, whereas t_{100} is the time at which the rheometer curve reaches its maximum value M_{HF}. Finally, it is interesting to notice that the scorching curve exhibits also a minimum point (coordinates: $t_m - M_m$), reached soon during the experimentation in the rheometer.

3.2 Experimental data

The numerical algorithm proposed is based on the experimental use of rheometers following the ASTM D 2084 method [4] at different temperatures to collect a suitable database of experimental data regarding scorching curves (t_m, t_2, t_{90}, M_m, M_2, M_{HF}) at increasing temperatures and their successive interpolation by means of a simple mathematical formulation. The aim of the paper is to use the experimental-mathematical method proposed in the accelerated sulphur vulcanization for items with considerable thickness. In fact, a numerical approximation of the scorching curve at different temperatures is necessary to have a prediction of the degree of vulcanization of rubber during an industrial process. We can, indeed, have a prediction of the vulcanization process inferring mechanical properties simply passing from a scorching curve to another in the collected database. Values between experimental data collected are numerically simulated through linear interpolation.

At present, the knowledge regarding the chemistry of accelerated sulphur vulcanization is somewhat fragmented and confused.

In this framework, several useful experimental data are available in the literature from Poh [14–19], who observed a marked relation among scorching time, amount of activators used and rheometer temperatures.

However, data reported in the literature are insufficient to fully calibrate the numerical model here proposed. In fact, in order to predict the vulcanization rate during an industrial process of production of thick items, it is necessary to have at disposal from laboratory experimentation, several "characteristic points" of the rheometer curve for the same rubber receipt, at different controlled curing temperature inside the oscillating rheometer.

In particular, it is necessary to know (at least) the minimum point of the scorching curve, scorching time (with its torque value), t_{90} and torque value after full vulcanization. These values allow to post-process experimental results and approximate the scorching curve with simple mathematical functions (e.g. parabola and hyperbole, as shown in the previous sub section).

3.3 Mathematical approximation used in numerical simulations: validation

The mathematical approximation used to reproduce numerically a typical scorch curve is represented in Fig. 5, and it relies in approximating experimental data by means

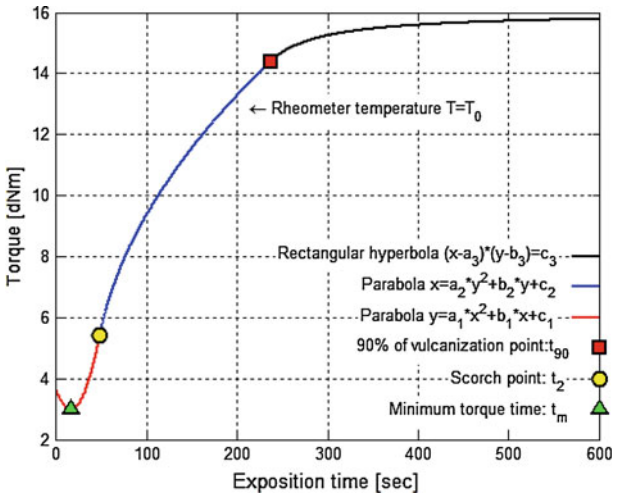

Fig. 5 Numerical three functions composite curve to simulate rheometer test

of a composite first derivative continuous curve represented by two parabolas and a rectangular hyperbola.

In particular, only three points of the experimental scorch curve are needed, for instance the minimum point (green triangle), the scorch point (yellow circle) and the t_{90} point. It is worth noting that, assuming by definition that t_{90} torque modulus is 90% of the torque of the vulcanized specimen, also horizontal asymptote of the rectangular hyperbola is known. Obviously a point different from t_{90} may also be selected, depending on the experimental information available and with the aim of approximating experimental curve as close as possible.

More in detail, equations of the composite mathematical scorch curve are the following:

$$\begin{aligned} M(t) &= a_1 t^2 + b_1 t + c_1 \\ t(M) &= a_2 M^2 + b_2 M + c_2 \\ (t - a_3)(M - b_3) &= c_3 \end{aligned} \tag{1}$$

Firstly, constants a_1, b_1 and c_1 are determined by imposing that the first parabola passes through the scorching point and has a minimum located at the experimental minimum of the scorching curve (two algebraic conditions).

Afterwards, the second parabola (with horizontal axis) is determined imposing the passage through the scorching point and assuming that first and second parabola have the same first derivative at the scorching point. This latter requirement, through the well known theorem of first derivative of the inverse function, reduces to the following condition:

$$2a_1 t_2 + b_1 = \frac{1}{2a_2 M_2 + b_2} \tag{2}$$

Finally, hyperbola is analytically determined imposing (1) the passage through e.g. t_{90}, (2) the common tangent in t_{90} with the second parabola and (3) assuming a horizontal asymptote equal to M_{HF}.

Obviously, some approximations are introduced with the composite analytical approach here proposed, but the numerical procedure seems particularly attractive, since only few points (3 points and an asymptotic value) are need to have a reliable estimation of the scorching curve of the compound under consideration.

The physical interpretation of the use of a three functions composite curve is the following: the first parabola corresponds to a viscous status of the compound before the vulcanization is started, the second curve represents the fast curing process (e.g. allylic substitution, crosslinking precursion formation, crosslinking reaction), whereas the last curve is the combination of the second step with oxidation, desulphuration and devulcanization.

In order to test the reliability of the numerical approach here proposed (which will be used to estimate point by point the degree of vulcanization of a real rubber item), four experimental scorching curves collected from Henning [20] are here considered. Experimental cure curves correspond to four different compounds in which zinc salts at molar equivalency 5.0 phr zinc oxide, 12.8 phr ZDA, 14.5 phr ZDMA, 10.4 phr ZMMA are used as activators. Rubber used is Goodyear Natsyn 2200® and the reader is referred to Henning [20] for a detailed description of the compound.

ZDA indicates a zinc diacrylate produced by Sartomer (Sartomer SR705), ZDMA is a zinc di-metacrylate (Sartomer SR708), whereas ZMMA is a zinc mono-metacrylathe (Sartomer SR709).

Scorching time and values of torque to use in the numerical approximation of the experimental data are collected from Henning [20]. Experimental scorching curves are obtained at 160° following ASTMD 2084 [4], using an arc deflection of 3°. In Fig. 6, a full comparison between experimental data provided using the four activators analyzed and the numerical approximation here proposed is represented. As it is possible to notice, in all the cases analyzed a satisfactory agreement is obtained, for all the vulcanization times inspected. Despite the fact that, as obvious, reversion can non be reproduced with the approach here proposed, and a more complex approximation is need, the agreement is in any case very good.

In order to predict input parameters for the optimal vulcanization of thick items, it is however necessary to have at disposal scorching curves of the same compound at different temperatures. Such curves (or only meaningful points) are collected in a database and fitted numerically with the procedure proposed.

In this framework, some results of a limited experimental program regarding scorching tests on a commercial rubber compound at different temperatures have been collected and used in the numerical simulations. Following our own experience in this field, we have considered a commercial EPDM (Dutral TER 4047 produced by Polimeri Europa) with the following characteristics: 40% in weight of Propylene content, Mooney viscosity (1+4) at 125 °C equal to 55 and 4.5 % weight of ENB (5-ethyliden-2-norbornene). The evaluated blend have been prepared without trouble in a 13 lt. internal mixer through upside down method at 80–90 °C.

The composition was the following: Polymer 100 phr, filler carbon black(N 330) 60 phr, Zinc oxide 5 phr, plasticizer paraffinic oil (cortis 100M) 50 phr, stearic acid 1

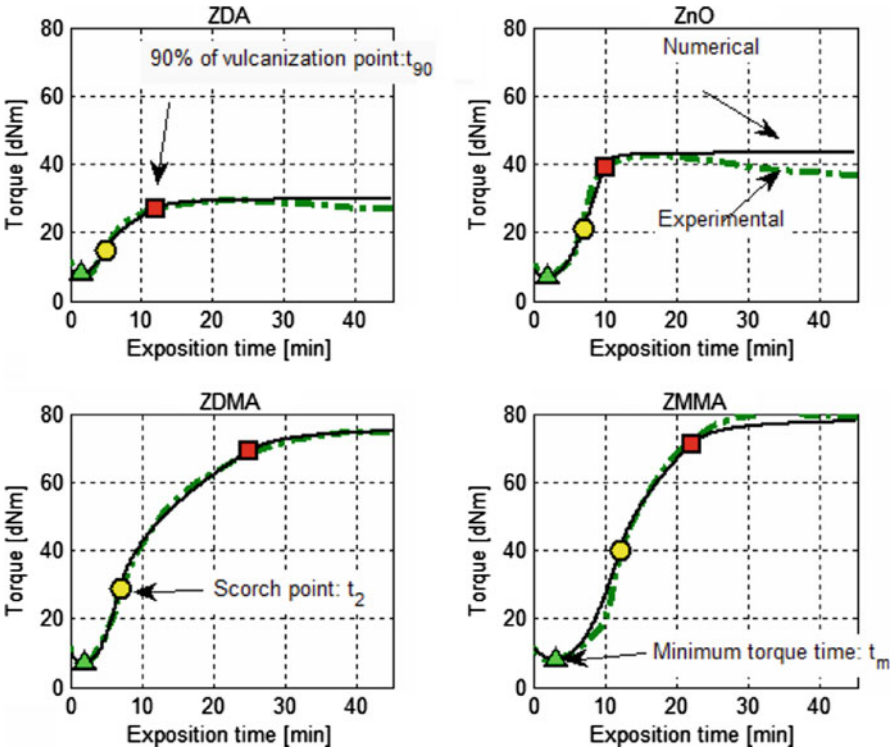

Fig. 6 Comparison between experimental data [20] and the numerical three functions curve proposed

Table 1 Rheometer output data obtained for Dutral TER 4047 blend at three different imposed temperatures

Temperature T(°C)	200	180	160
t_2—scorch time (s)	48	84	152
t_{90}—90% vulcanization time (s)	237	380	720

phr, 2-mercaptobenzothiazole 0.8 phr, tetramethylthiuram disulfide 0.8 phr, zinc dibutyldithiocarbamide 2 phr, sulphur 2 phr and Mooney viscosity (1 + 4) at 100 °C equal to 40. The blend was analyzed in an oscillating Die Rheometer (ODR) according to ASTM D 2084 at 160, 180 and 200 °C using an arc deflection of 3°. The characteristic times t_2 and t_{90} at the different temperatures inspected are summarized in Table 1.

The vulcanization was carried out by compression press at 200 °C for 450 s, at 180 °C for 900 s and at 160 °C for 1,800 s. All items vulcanized were tested in terms of tensile strength, elongation and tension set at 100% of elongation after 24 hours at room temperature following the ASTM D412-83, D624-86 and D4482-85 [21,22]. Output data are collected in Table 2. Finally, in Table 3, rheometer torque relative to the minimum point, the scorching point and t_{90} are summarized.

From data collected in Tables 1 and 3, the mathematical approximation of the scorching curves at different temperatures reported in Fig. 7 have been obtained with

Table 2 Output mechanical properties obtained for Dutral TER 4047 blend at three different imposed temperatures

Temperature T(°C)	200	180	160
σ_t— tensile strength (MPa)	14.6	15.8	13.0
$\varepsilon_{\%}$— elongation %	480	520	460
Tension set %	5	5	5

Table 3 Rheometer torque obtained for Dutral TER 4047 blend at three different imposed temperatures

Temperature T(°C)	200	180	160
Minimum torque M_m (dNm)	4.2	6.7	10.0
Scorch torque M_2 (dNm)	9.2	11.7	15.0
Asymptote torque M_{HF} (dNm)	45	46	4

the model proposed. Such curves will be used in the following section to predict the optimal vulcanization of a thick item industrially produced.

3.4 Cured rubber tensile strength

The evaluation of the level of vulcanization of a rubber compound is usually determined a-posteriori through the macroscopic evaluation of mechanical properties of the items produced industrially at the end of the vulcanization process.

There are several standard parameters that can be measured, as for instance tear resistance, tensile strength, tension set, etc. [21,22].

From a theoretical and practical point of view, to link the vulcanization process with mechanical properties of rubber is not an easy task.

Experimental tests conducted on EPDM rubber vulcanized with accelerated sulphur (see for instance Henning [20]) show that a numerical relation between rubber macroscopic mechanical properties (tear resistance, tensile strength, Young modulus, etc.) and torque modulus after curing (or more precisely, the increase of the torque ΔM which measures the increase in the torque obtained at the end of the vulcanization) exists.

In Fig. 8, the experimental relation between ΔM and output properties (a: tensile strength, b: 100% modulus, c: elongation, d: tear strength) obtained by Henning [20] is represented, along with numerical experimental data fitting (interpolation with polynomial of degree 3).

As it is possible to notice, some of the output properties exhibit a non linear behavior with possible decrease increasing ΔM, obviously due to an over-vulcanization of the specimens.

For the sake of conciseness, in the numerical simulations reported in what follows, we consider as output parameter to optimize rubber tensile strength, but no conceptual differences occur considering other quantities.

In particular, the numerical relation between ΔM and tensile strength depicted in Fig. 9 is used in the simulations. Such relation refers to some experimental data avail-

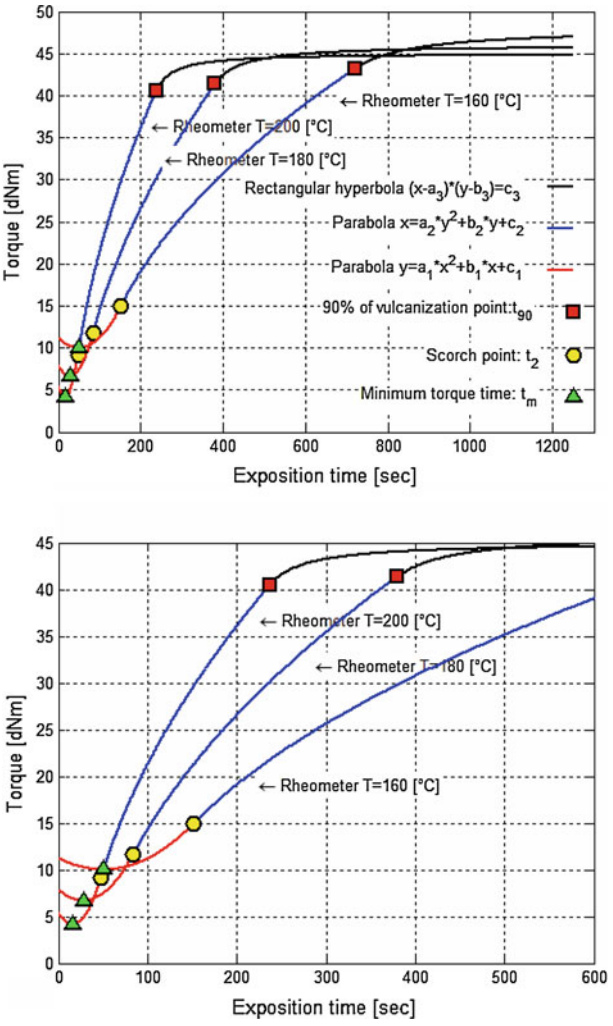

Fig. 7 Rheometer numerical curves at increasing controlled temperatures (Dutral TER 4047)

able for the commercial compound Dutral TER 4047 (experimental values of output tensile strength are also reported in Table 2).

Another important aspect to underline is that, obviously, the representation of Fig. 9 is able to give correct information on output parameters only at constant temperatures (note that $T \neq T_n$, being T rubber temperature), i.e. results can non be applied directly to a rubber infinitesimal element subjected to curing, because its temperature changes continuously at successive time steps.

As well known, in fact, real non constant temperature profiles $T = T(\mathbf{P}, t)$for each point $\mathbf{P}$ of the element to vulcanize have to be determined solving a suitable differential system, as it will be shown in what follows. Nonetheless, Fig. 9 gives a precise (although approximate) idea of the complex behavior of rubber during vulcani-

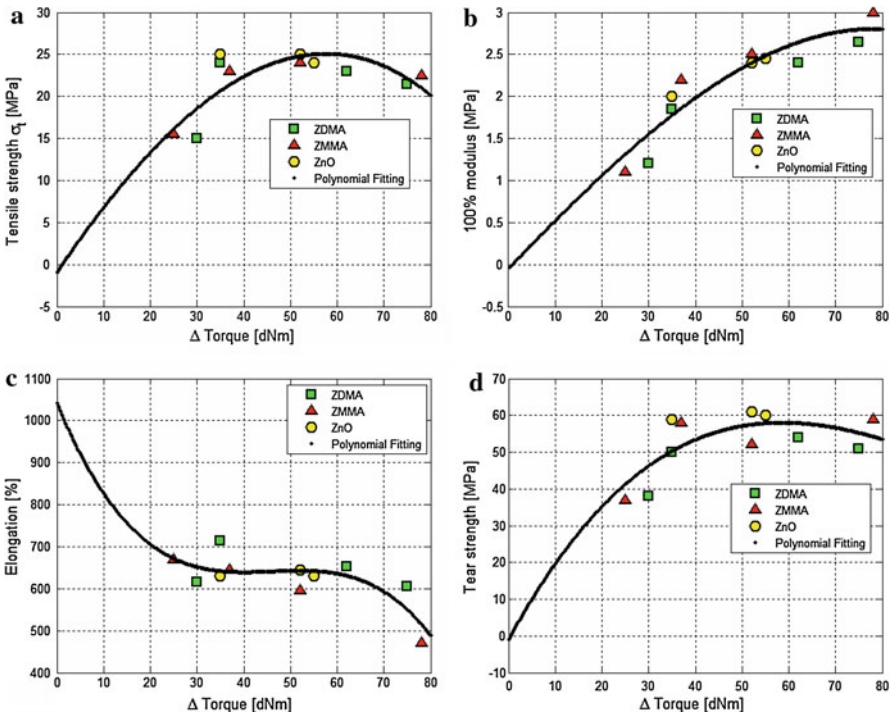

Fig. 8 Relation between output mechanical properties and rheometer curves. **a** Tensile strength. **b** 100% modulus. **c** Elongation. **d** Tear strength

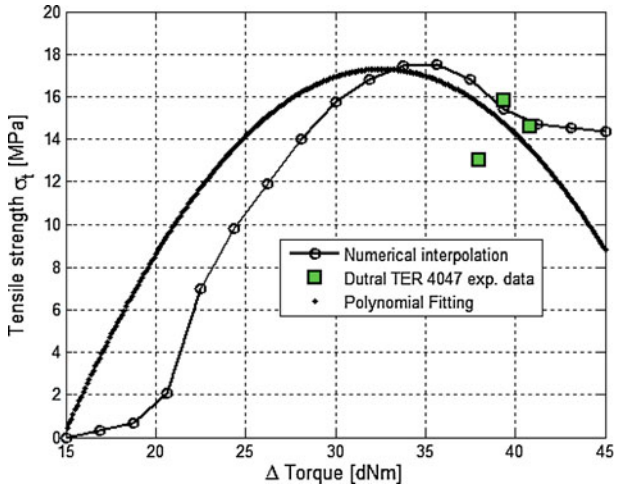

Fig. 9 Numerical relation between tensile strength σ_t and ΔM used in the simulations regarding the industrial process optimization (Dutral TER 4047 rubber compound)

zation, addressing that a strong variability of output mechanical properties is obtained changing curing time and vulcanization temperature.

4 Kernel of the numerical model adopted

In this section, the basic features of the numerical approach utilized for the optimization of complex 2D/3D rubber thick elements is outlined. The pseudo-code of the algorithm used for the optimization process is summarized in Fig. 10.

Essentially, the following blocks are repeated in the code at different T_n or exposition times:

1) Determination of temperature profiles for each point of the item (i.e. node in the FEM mesh). At this aim, heat transmission Fourier's law in 2D/3D dimensions [7–13,23] is utilized. Since in the most general case, Fourier's equation is partial and differential, a finite element (FEM [24]) strategy is implemented [25] to solve the problem.

2) Determination, for each point of the object, of its final mechanical properties at different temperatures and different exposition times. An optimal vulcanization

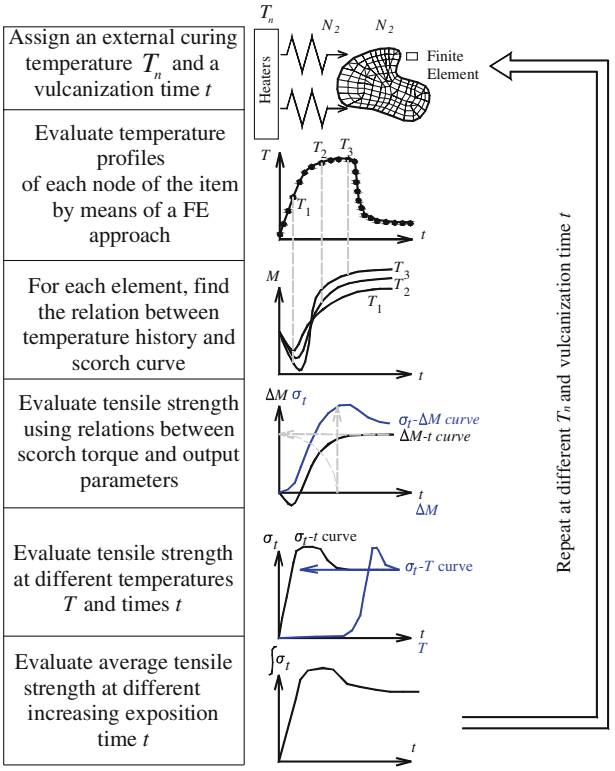

Fig. 10 Schematic representation of the optimization process phases

time at different insulator fixed temperatures exists, where objective function (tensile stress, elongation, tear strength, etc.) is maximized. Since we are interested in evaluating the overall properties of the vulcanized rubber, an averaged objective function is adopted (i.e. the mean tensile strength is maximized).

3) Determination, by means of a simple alternating tangent (AT) procedure of optimal (T_{ni} t_i) input pairs where output mechanical properties are maximized. The AT method [26] requires to proceed through sections in which T_n or t are fixed, in bounding the remaining undetermined variable at the first iteration, in evaluating tensile strength first derivatives at the extremes and at the middle point of the interval inspected and in bisecting iteratively the interval on the base of first derivative sign.

4.1 Governing partial differential equations

The vulcanization process can be schematically subdivided into two separate phases: in the first, elastomers are exposed to high temperatures in order to activate cross-linking and thus vulcanization, followed by a second cooling phase (usually with air or water) in which rubber is kept to ambient temperature.

Let us consider a generic rubber three dimensional object, in which the coefficient of thermal conductivity λ_p, specific heat c_p^p and density ρ_p are regarded as constant. Temperature profiles for each point of the element are obtained solving numerically a partial differential equations system problem. Fourier's heat equation law is used [23]. In particular, the heat balance field equation is the following:

$$\rho_p c_p^p \left(\frac{\partial T}{\partial t}\right) - \lambda_p \nabla^2 T - r_p \Delta H_r = 0 \tag{3}$$

where

– ρ_p, c_p^p and λ_p are EPDM density, specific heat capacity and heat conductivity respectively;

– ΔH_r is rubber specific heat (enthalpy) of reaction and is expressed in kJ/mol;

– r_p is the rate of cross-linking and is expressed in mol/$\left(\mathrm{m}^3\mathrm{s}\right)$.

It is worth noting that the term $r_p \Delta H_r$ in Eq. (3) is the heat required by the vulcanization reactions, see Fig. 1. ΔH_r, usually ranges from 120 to 180 kJ/mol. $r_p \Delta H_r$ depends on both T and t and several models can be used for an analytical definition of r_p function. Nonetheless, for the sake of simplicity we assume here a constant value for r_p. More complex relations can be adopted [12] in the model proposed without any numerical difficulty. In any case, the contribution of such term in the heat exchange Eq. (3) is negligible.

4.2 Initial and boundary conditions

When heat transmission at the external boundary is due to convection + radiation (extrusion process), the following boundary conditions must be applied:

$$\lambda_p \frac{\partial T\left(\mathbf{P}, t\right)}{\partial \mathbf{n}\left(\mathbf{P}\right)} + h\left(T\left(\mathbf{P}, t\right) - T_n\right) + q_{rad} = 0 \tag{4}$$

where

- h is the heat transfer coefficient between EPDM and vulcanizing agent at fixed temperature T;
- T_n is vulcanizing agent (e.g. nitrogen) temperature;
- $\mathbf{P}$ is a point on the object surface and $\mathbf{n}$ is the outward versor on $\mathbf{P}$;

q_{rad} is the heat flux transferred by radiation. Radiation contribution for the vulcanization of complex 2D geometries may not be determined precisely. At a first glance, the simplified following formula is applied:

$$q_{rad} = \sigma\left(T_n^4 - T\left(R_p, t\right)^4\right) \Big/ \left[1/\varepsilon_p + \frac{A_p}{A_n}\left(1/\varepsilon_n - 1\right)\right] \tag{5}$$

where

- $\sigma = 5.67 \cdot 10^{-8} \frac{W}{m^2 K^4}$ is the Stefan-Boltzmann constant;
- $\varepsilon_{p,n}$ are emissivity coefficients;
- $A_{p,n}$ are the areas of heat exchange (p: rubber item, n: curing agent).

For the cooling phase, no differences occur with respect to the curing process, provided that the temperature of the cooling agent is known at increasing time steps.

In particular, heat exchange during the cooling phase occurs basically for convection, i.e. following the partial differential equation:

$$\lambda_p \frac{\partial T\left(\mathbf{P}, t\right)}{\partial \mathbf{n}\left(\mathbf{P}\right)} + h_w\left(T\left(\mathbf{P}, t\right) - T_w\right) = 0 \tag{6}$$

where h_w is the water (air) heat transfer coefficient, T_w is the water (air) cooling temperature and all the other symbols have been already introduced.

Initial conditions on temperatures at each point at the beginning of the curing process are identically equal to the ambient temperature (hereafter fixed equal to 35 °C for the sake of simplicity), whereas initial conditions at the beginning of the cooling phase are obtained from the temperature profiles evaluated at the last step of the cooling zone, i.e. at $T\left(\mathbf{P}, t_c\right)$, where t_c is the total curing time and $\mathbf{P}$ is a generic point belonging to Ω.

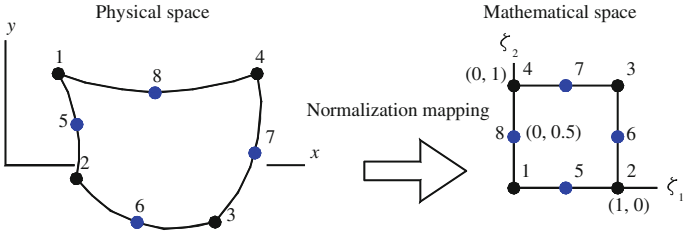

Fig. 11 Eight-noded plane elements used for the 2D thermal transient analyses (*left* physical space, *right* mathematical space)

4.3 Finite element (FE) implementation: eight-noded elements (2D case)

Partial differential equations system (3–6) for complicated geometries and non uniform initial temperature conditions can not be solved in closed-form. Therefore, in what follows, a Finite Element (FEM) [9,10,23] discretization of the domain is utilized to obtain a reliable approximation of temperatures at each element point and at successive time steps. The procedure has been completely implemented in Matlab [25] language. In this way, resultant FE temperature profiles at each time step are directly collected from the numerical analysis and utilized for the evaluation of output rubber mechanical properties by means of an integrated tool.

When dealing with a generic extruded 2D rubber item, 8-noded plane elements have been used, see Fig. 11. Temperature field interpolation is assumed polynomial inside each element, i.e.:

$$T\left(\mathbf{P}\right) = \mathbf{N}^e \mathbf{T}^e \tag{7}$$

where

- $\mathbf{T}^e = \left[T^1 \; T^2 \; \ldots \; T^8 \right]^T$ is the vector of nodal temperatures;
- $\mathbf{N}^e = \left[N^1 \; N^2 \; \ldots \; N^8 \right]$ is the vector of so-called shape functions N^i $(i = 1, \ldots, 8)$;
- $\mathbf{P}$ is a point of coordinates x_P, y_P and z_P inside the element.

Indicating with $\mathbf{X}_i = (x_i, y_i, z_i)$ elements nodes coordinates, N^i are expressed by the following relation:

$$\mathbf{X} = \sum_{i=1}^{8} N_i \left(\xi_1, \xi_2, \xi_3\right) \mathbf{X}_i$$

$$N^i = \begin{cases} \frac{1}{4}\left(1+\xi_1^i\xi_1\right)\left(1+\xi_2^i\xi_2\right)\left(\xi_1^i\xi_1+\xi_2^i\xi_2-1\right) & i = 1,2,3,4 \\ \frac{1}{2}\left(1-(\xi_1)^2\right)\left(1+\xi_2^i\xi_2\right) & i = 5,6 \\ \frac{1}{2}\left(1-(\xi_2)^2\right)\left(1+\xi_1^i\xi_1\right) & i = 7,8 \end{cases} \tag{8}$$

where $\xi_i \in [0\ 1]$ is a normalized coordinate and vertices are obtained alternatively imposing $\xi_j = 1$ and $\xi_i = 0$ and vice-versa.

In the numerical simulations reported, the following parameters have been used: EPM/EPDM density $\rho_p = 922\,\mathrm{Kg/m}^3$, rubber specific heat capacity $c_p^p = 2{,}700\,\mathrm{J/(kg\,^\circ C)}$, $\lambda_p = 0.335\,\mathrm{W/(m\,^\circ C)}$, $\Delta H_r = 180\,\mathrm{kJ/mol}$, water heat transfer coefficient $h_w = 1{,}490.70\,\mathrm{W/(m^2\,^\circ C)}$, curing agent heat transfer coefficient $h = 900\,\mathrm{W/(m^2\,^\circ C)}$, $\varepsilon_p = 0.60$, $\varepsilon_c = 0.70$, water cooling temperature $T_w = 25\,^\circ\mathrm{C}$.

As a rule, h_w and h should be derived from well known empirical formulas related to laminar/turbulent flow of fluids, see [12] for details, nevertheless here characteristic values are used for the sake of simplicity.

The geometry of the 2D rubber item analyzed in this paper is sketched in Fig. 12. In Fig. 13, color patches representing temperature profiles obtained during a FEM simulation at increasing instants are represented ($T_n = 180\,^\circ\mathrm{C}$ is assumed). As it is

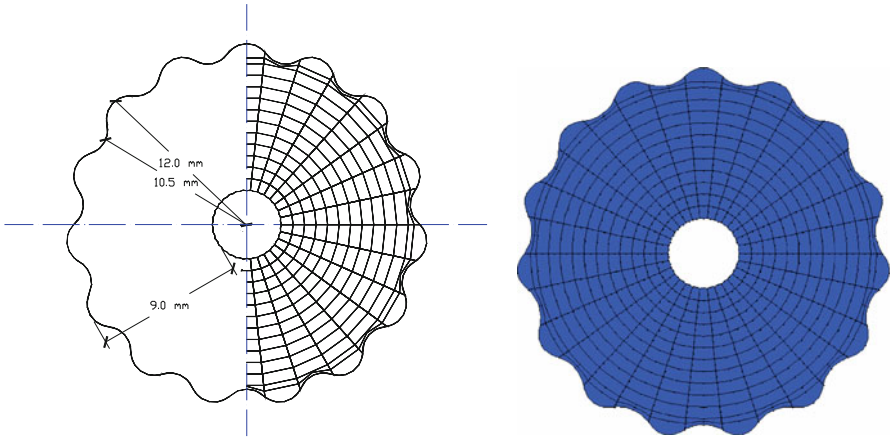

Fig. 12 Geometry and FEM discretization by means of eight noded elements (1230 nodes, 390 plates)

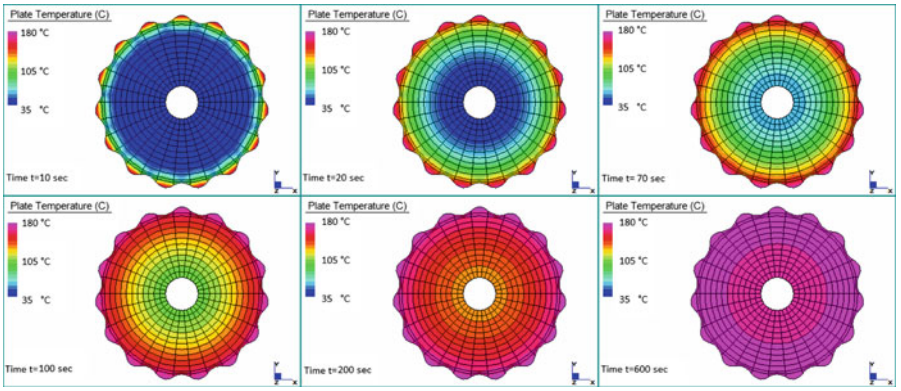

Fig. 13 Snapshots from the FEM program representing temperature profiles at increasing exposition times ($T_n = 180^\circ\mathrm{C}$)

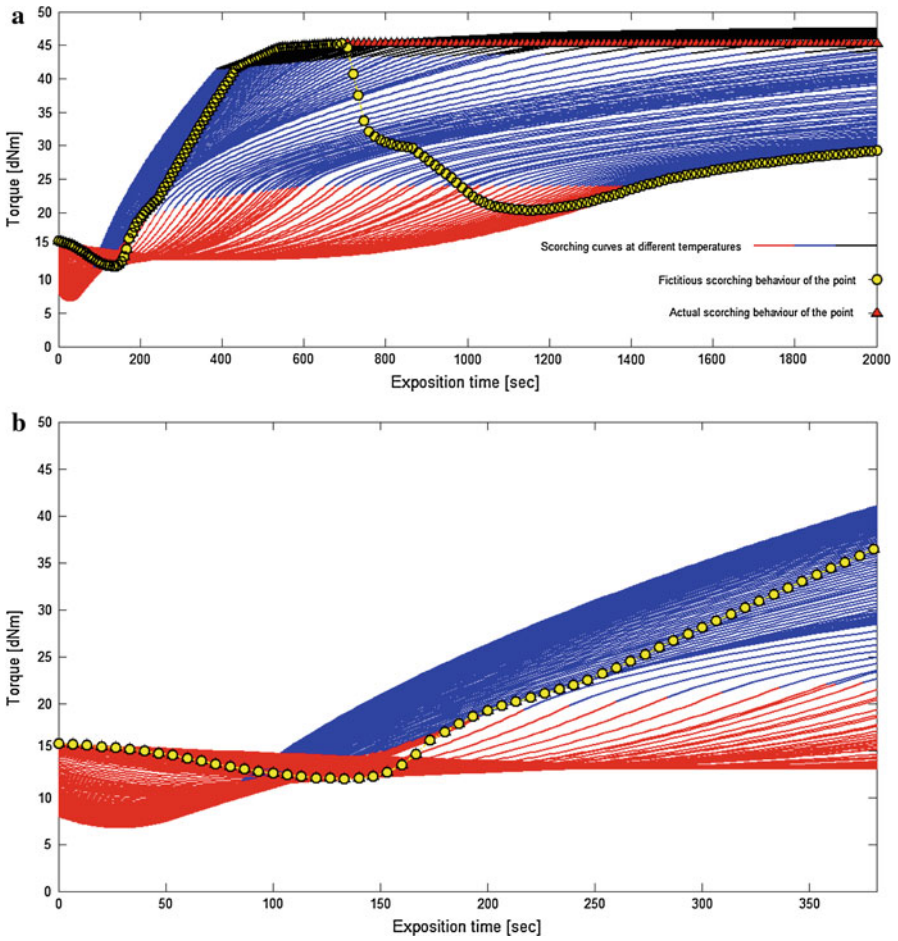

Fig. 14 Point A behavior during vulcanization, passage from *low* temperature to *high* temperatures scorching curves. **a** behavior during all the vulcanization process. **b** detail in the first phase of the vulcanization

possible to notice, internal points heating is sensibly slower with respect to the skin, thus influencing the quality of the vulcanization to a great extent.

The vulcanization behavior of a point belonging to the internal surface of the item (hereafter called Point A) is represented in Figs. 14 and 15. In particular, in Fig. 14, the path followed by Point A during vulcanization in an "ideal" rheometer diagram is represented. To fully understand Fig. 14, it is necessary to consider the temperature profile which undergoes Point A, represented in Fig. 15 (bottom-right). Initially, Point A temperature increases, and thus Point A passes from rheometric curves at low temperatures to rheometric curves at high temperatures. Such curves are numerically interpolated, as already pointed out, from experimental data available for the rubber compound inspected, see Fig. 7.

When the maximum temperature is reached, Point A follows the rheometric curve relative to such temperature, stabilizing its behavior at increasing times on that rheometer curve.

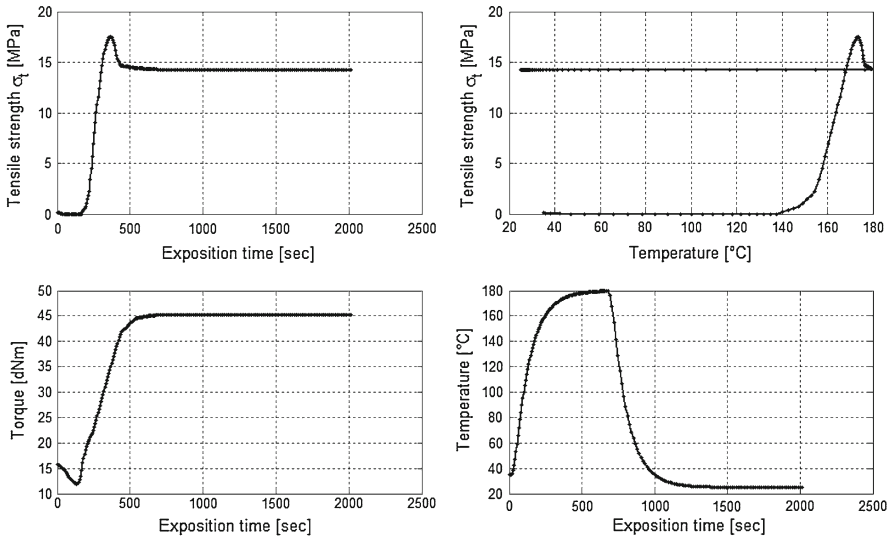

Fig. 15 Point A mechanical properties evolution during vulcanization. *Top-left* exposition time-tensile strength diagram. *Top-right* temperature-tensile strength diagram. *Bottom-left* exposition time-torque diagram. *Bottom-right* temperature profile

When the curing finishes, temperature suddenly decreases. Here, two paths have to be monitored numerically for Point A, represented in Fig. 14 with circles and triangles. The numerical behavior represented by circles is not real, because it would be referred to a material without any memory of the vulcanization and relies in a compound which ideally continues to follow the rheometric curves at lower temperatures. On the contrary, the real behavior of the material under consideration is represented by the triangles, indicating that the level of vulcanization reached at the end of the curing process cannot be inverted reducing temperature, but can only be stopped.

Once that the path in the rheometric curve is known numerically for the point under consideration, tensile strength reached increasing exposition time can be easily determined through the relation sketched in Fig. 9. For point A, the exact vulcanization history in terms of $\Delta M - \sigma_t$ diagrams is represented in Fig. 15 (bottom-left). By means of point temperature profiles (obtained using FEM) and the rheometric path ($\Delta M - \sigma_t$ history), tensile strength reached by the point at increasing exposition times and at the different actual temperatures during the vulcanization process can be easily determined (Fig. 15 top diagrams).

The same considerations can be repeated for any point of the item, thus giving the possibility to evaluate the average final tensile strength. For instance, in Figs. 16 and 17, the behaviour during curing of a point near the external surface of the item (hereafter called Point B) is represented. From Fig. 16 it is rather evident that Point B reaches maximum vulcanization temperature more quickly with respect of Point A, since the scorch curves followed by the point are very near one each other. On the other hand, the cooling phase is somewhat clear in the diagram.

From a detailed analysis of point A and point B behaviour, it can be argued that a generalized over-vulcanization of the item has been obtained in this case, since the

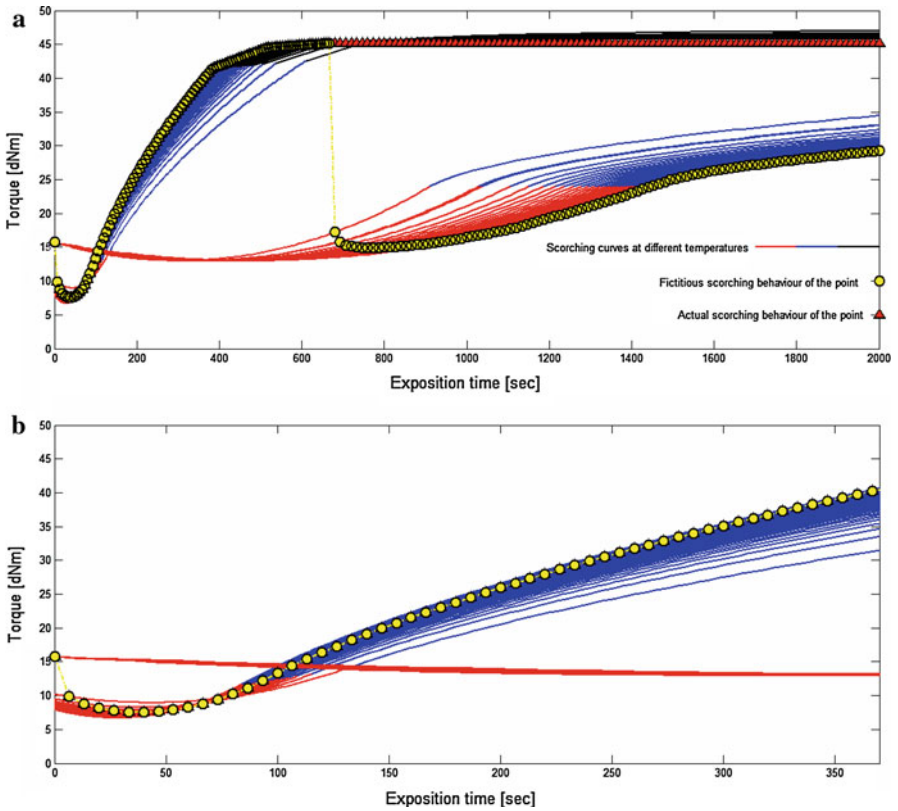

Fig. 16 Point B behavior during vulcanization. **a** behavior during all the vulcanization process. **b** detail in the first phase of vulcanization

maximum tensile strength is reached before the end of the curing process in both cases, with a consequent decrease of final mechanical properties at the end of the simulations.

5 A bisectional approach for optimal vulcanization

The alternating tangent approach used in this paper was originally developed by Milani and Milani [26] and the reader is referred there for a detailed description of the method used. The approach is based on the numerical evaluation of tensile strength first derivatives with respect to exposition time on several sections at fixed curing temperatures T_n and in the iterated bisection of a determined exposition time search interval.

At a fixed T_n temperature, Fig. 18, tensile strength is evaluated on the two extremes of the interval (points 1 and 2), usually placed at a very under-vulcanized and a very over-vulcanized exposition time.

First derivatives $d\sigma_t/dt$ of tensile strength with respect to exposition time are needed at the search interval extremes. Since $d\sigma_t/dt$ are not known analytically, a numerical procedure based on finite differences is adopted.

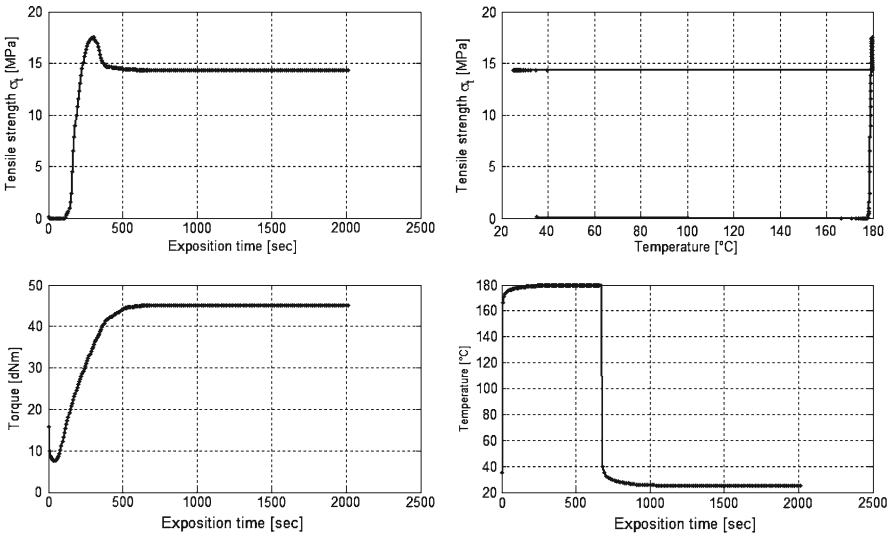

Fig. 17 Point B mechanical properties evolution during vulcanization. *Top-left* exposition time-tensile strength diagram. *Top-right* temperature-tensile strength diagram. Bottom-left: exposition time-torque diagram. *Bottom-right* temperature profile

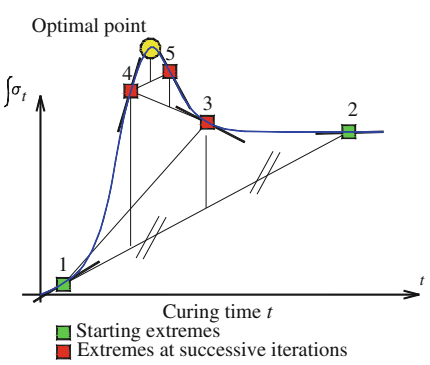

Step 0: evaluate first derivative at points 1 and 2
Step 1: evaluate first derivative at point 3 (mean value between abscissae 1 and 2)
Step 3: select the new extreme of the interval on the bases of the sign of 3 first derivative (negative 1-3 positive 3-2)
Step 4: repeat Step 1 substituting original points with the new extremes

Fig. 18 Alternating tangent approach (AT) basic scheme

A point $1'$ with exposition time equal to 1 plus a small increment Δt and a point $2'$ with exposition time equal to 2 decremented of a small Δt are considered. Tensile strength is then evaluated in $1'$ and $2'$, thus giving the possibility to evaluate first derivatives at 1 and 2. By definition, numerical first derivative at points 1 and 2 is given by the following equation:

$$\left.\frac{d\sigma_t}{dt}\right|_1 = \frac{\sigma_t|_{1'} - \sigma_t|_1}{\Delta t}$$
$$\left.\frac{d\sigma_t}{dt}\right|_2 = \frac{\sigma_t|_2 - \sigma_t|_{2'}}{\Delta t} \tag{9}$$

where the symbol $x|_i$ indicates that the quantity x is numerically evaluated at point i.

Δt is usually fixed in the range 1–3 s to obtain reliable results.

Middle point first derivative of the search interval is also needed, as depicted in Fig. 18.

Once that first derivatives are at disposal on the search interval extremes and on the middle point, a bisection procedure is adopted, reducing the search interval to one-half. In particular, the new interval is respectively the right or the left one half depending on the sign of first derivatives of the extremes with respect to the middle point one, i.e.

$$\begin{aligned} &\text{if } \left.\frac{d\sigma_t}{dt}\right|_1 \cdot \left.\frac{d\sigma_t}{dt}\right|_3 \geq 0 \rightarrow \text{select right semi} - \text{interval} \\ &\text{if } \left.\frac{d\sigma_t}{dt}\right|_2 \cdot \left.\frac{d\sigma_t}{dt}\right|_3 \geq 0 \rightarrow \text{selectleft semi} - \text{interval} \end{aligned} \tag{10}$$

The procedure is repeated iteratively on the new half-interval, bounding more and more strictly the actual optimal solution at the new iteration. The algorithm is stopped until a desired degree of accuracy is obtained (circle in Fig. 18).

It is worth noting that the procedure proposed converges also at fixed exposition times and varying nitrogen temperature T_n, therefore numerical simulations can be performed using two "perpendicular" different strategies.

6 Numerical simulations

A set of numerical simulations is reported in this section, in order to show the capabilities of the experimental-numerical procedure proposed. Numerical results refer to the temperatures database collected from the FEM model of Fig. 12. In particular, several thermal analyses have been performed changing curing temperature T_n and exposition time t.

Optimal input parameters functions $\hat{T} = \hat{T}\,(T_n, t) = 0 | \hat{T} \equiv \left\{ P^i = \left(T_n^i, t^i\right) \text{optimal} \right\}$ are obtained through the approach proposed.

In particular, optimal $\hat{T}$ curves (expressed as implicit functions in T_n and t) are numerically evaluated solving the following optimization problem through bisection, once that one of the input parameters T_n^i or t^i is a priori fixed (sectional approach):

$$\begin{aligned} &\max \frac{1}{N_L} \sum_{k=1}^{N_L} \sigma_t^k \left(T_n^i, t^i\right) \\ &\text{subject to} \begin{cases} T_n^i = \text{fixed} \\ t^{\min} < t^i < t^{\max} \end{cases} \\ &\text{PDEs system} \begin{cases} \rho_p c_p^p \left(\frac{\partial T}{\partial t}\right) - \lambda_p \nabla^2 T - r_p \Delta H_r = 0 \\ \text{boundary and initial conditions} \end{cases} \end{aligned} \tag{11}$$

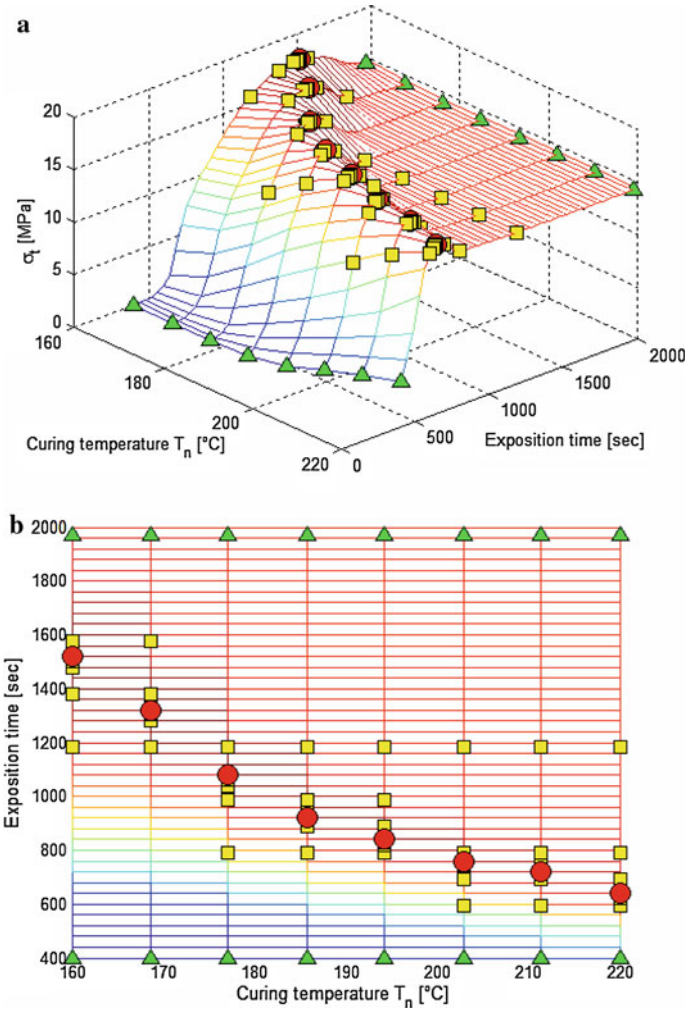

Fig. 19 2D extruded item. Optimal output tensile strength at different values of exposition time and nitrogen temperature. **a** 3D view. The surface represents results from the grid method, whereas *squares*, *triangles* and *circles* represent AT approach results. *Circles* are final optimized points form AT approach, squares extremes of the successive intervals inspected, *triangles* initial search intervals. **b** aerial view of optimized results

where N_L is the number of nodes in which the item is discretized and $t^{\min}$ ($t^{\max}$) is a lower (upper) bound limitation for curing temperature.

Results provided by the alternating tangent approach proposed are compared with those obtained subdividing $T_n - t$ plane with a regular grid. In the latter case, for each point $P^{i,j} \equiv \left(T_n^i, t^j\right)$ of the grid a mixed algebraic-PDEs system has to be solved:

$$\sigma_t = \frac{1}{N_L} \sum_{k=1}^{N_L} \sigma_t^k \left(T_n^i, t^j\right)$$

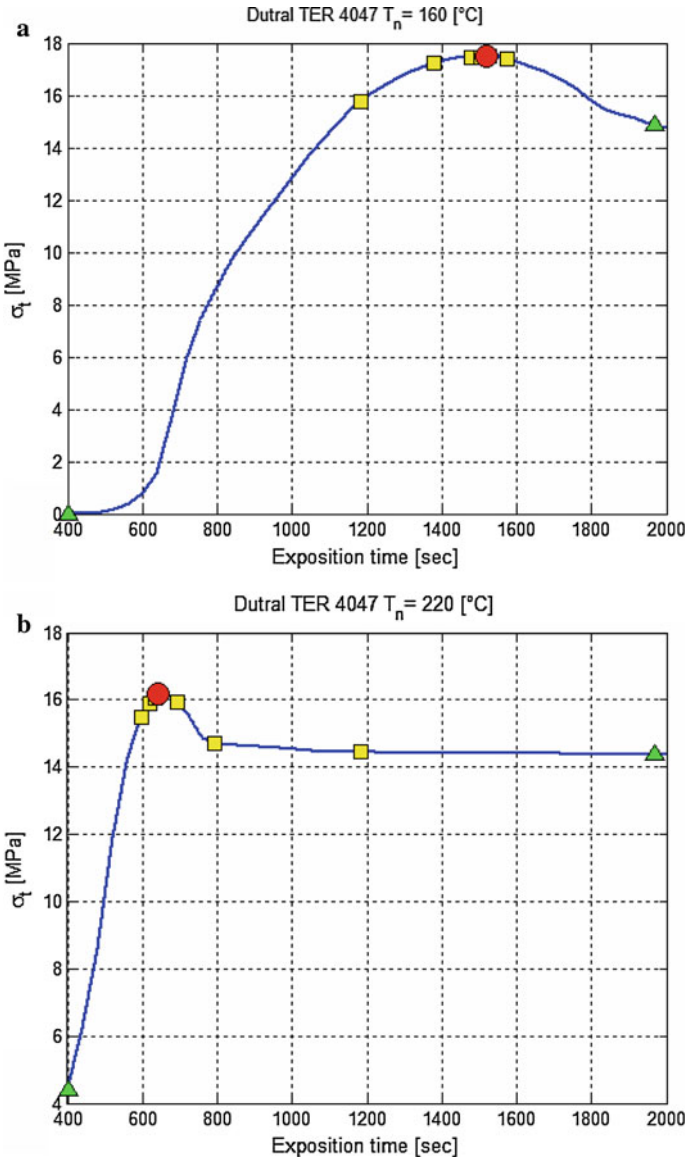

Fig. 20 2D vulcanized item. Optimal output tensile strength at different values of exposition time and fixed value of curing temperature. **a** $T_n = 160°C$. **b** $T_n = 220°C$. The *continuous lines* represent results from the grid method, whereas *squares*, *triangles* and *circles* represent AT approach results

$$\text{PDEs system} \begin{cases} \rho_p c_p^p \left(\frac{\partial T}{\partial t}\right) - \lambda_p \nabla^2 T - r_p \Delta H_r = 0 \\ \text{boundary and initial conditions} \end{cases} \tag{12}$$

Obviously a very large computational effort is required in solving problem (12), especially for very refined discretizations (as those needed in the present simulations) using

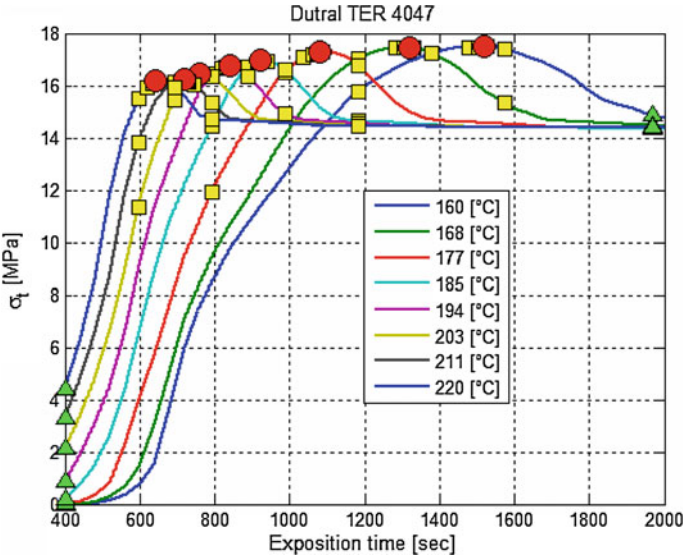

Fig. 21 2D vulcanized item. Optimal output tensile strength at different values of exposition time and fixed value of curing temperature. Simulations from 160°C to 220°C. The *continuous lines* represent results from the grid method, whereas *squares*, *triangles* and *circles* represent AT approach results

the grid method (otherwise a global optimization algorithm where objective function is not analytically known has to be performed).

In Fig. 19, rubber mean tensile strength at different temperatures and exposition times is reported for the problem at hand, assuming as compound to vulcanized Dutral TER 4047. The 3D surface is obtained with an expensive regular grid of points obtained solving (12) using FEM, whereas circles represent the optimal point obtained with the bisectional approach. Squares represent successive intervals extremes, whereas triangles the initial intervals. As can be argued from the figures, the speed up obtained with the algorithm adopted is remarkable. In this case, simulations are performed fixing curing temperature and bisecting exposition time.

In Fig. 20, results for two fixed curing temperatures (160° and 220°) and varying exposition time are reported. The continuous curve is an expensive section obtained with the grid method, with a grid of 10,000×10,000 points. A very refined grid is needed because peaks may be very narrow. Circles, squares and triangles are bisectional iterated solutions.

As a matter of fact, due to the item thickness, considerable differences on optimal points are observed varying curing temperatures in a wide range. A comparison regarding optimal points obtained increasing curing temperature from 160° to 220° with a step equal to 8–9 °C is depicted in Fig. 21.

The technical usefulness of Figs. 19 and 21 is worth noting. In particular, once that a certain compound with fixed scorch curves at different temperatures is chosen, producers can enter in the figures with a desired curing temperature (exposition time) and exit with the optimal exposition time (curing temperature) for the production line.

7 Conclusions

A numerical procedure for the determination of optimal input parameters (curing temperature and exposition time) for 2D thick poly-diene and EPDM rubber items vulcanized with accelerated sulphur has been presented. Vulcanization external temperature T_n and rubber exposition time t have been assumed as production parameters to optimize.

Objective function is represented by rubber final mean tensile strength after vulcanization. Despite the fact that the analyses presented are limited only to the utilization of two input variables and one output mechanical property, the algorithm proposed can be applied without any conceptual difficulty in a more general framework.

In the paper, a numerical model to fit experimental rheometers data based on a simple composite three functions curve, able to describe the increase of the viscosity at successive curing times at different controlled temperatures to use during the production of thick items vulcanized with sulphur has been used to evaluate crosslinking.

It is believed that rheometer curve is able to give an indirect information on the rubber reticulation kinetic at different temperatures, to use in a successive step to establish simplified analytical kinetic formulas to adopt in the accelerated sulphur vulcanization of poly-diene and EPDM elastomers.

In the model, some real rheometer curves at different specimen temperatures have been collected in order to follow step by step vulcanization in industrial practice, which occurs at variable temperatures during curing, with considerable differences from the core to boundary of the item.

Once that rheometer curves have been suitably collected in a database, they have been used to predict the optimal vulcanization of real items industrially produced.

A meaningful example of engineering interest, consisting of a thick 2D EPDM cylinder has been finally illustrated to validate the model proposed. For the case analyzed, the efficiency of the numerical procedure proposed has been demonstrated.

References

1. C. Goodyear, US Patent 3633 (1844)
2. F.W. Billmeier Jr., *Textbook of Polymer Science*, 3rd edn. (Wiley, New york, 1984)
3. M.L. Krejsa, J.L. Koenig, Rubber Chem. Technol. **66**, 376 (1993)
4. ASTM D 2084-81, *Standard Test Methods for Vulcanized Rubber and Thermoplastic Elastomers-Tension*. (Annual Book of ASTM Standards, Philadelphia 1986)
5. A.Y. Coran. Vulcanization, in *Science and Technology of Rubber (Chapter 7)* (Academic Press, New York, 1978)
6. M. Morton (ed.), *Rubber Technology*, 2nd edn. (Van Nostrand Reinhold, New York, 1981)
7. G. Milani, F. Milani, J. Math. Chem. **47**, 229–267 (2010)
8. G. Milani, F. Milani, J. Appl. Polym. Sci. **111**, 482–507 (2009)
9. Y. Jia, S. Sun, S. Xue, L. Liu, G. Zhao, Polymer **44**, 319–326 (2002)
10. Y. Jia, S. Sun, S. Xue, L. Liu, G. Zhao, Polymer **43**, 7515–7520 (2002)
11. X. Wang, Y. Jia, L. Feng, L. An, Macromol. Theory Simul. **18**, 336–354 (2009)
12. V. Kosar, Z. Gomzi, Thermochim. Acta **457**, 70–82 (2007)
13. V. Kosar, Z. Gomzi, K. Sintic, Chem. Eng. Process. **46**, 83–88 (2007)
14. B.T. Poh, K.W. Wong, J. Appl. Polym. Sci. **69**, 1301–1305 (1998)
15. B.T. Poh, C.C. Ng, Eur. Polym. J. **34**, 975–979 (1998)
16. B.T. Poh, M.F. Chen, B.S. Ding, J. Appl. Polym. Sci. **60**, 1569–1574 (1996)

17. B.T. Poh, C.S. Te, J. Appl. Polym. Sci. **74**, 2940–2946 (1999)
18. B.T. Poh, E.K. Tan, J. Applied Polym. Sci. **82**, 1352–1355 (2001)
19. B.T. Poh, H. Ismail, K.S. Tan, Polym. Test. **21**, 801–806 (2002)
20. S.K. Henning, The use of coagents in sulfur vulcanization: functional Zinc Salts, in *Proceedings of the Spring 167th Technical Meeting of the Rubber Division*, American Chemical Society, San Antonio, TX, 16–18 May 2005
21. L. Bateman (ed.), *The Chemistry and Physics of Rubber-Like Substances* (MacLaren, London, 1963)
22. ASTM D412-83, D624-86, D4482-85, *Standard test methods for vulcanized rubber and thermoplastic elastomers-tension* (Annual Book of ASTM Standards, Philadelphia, 1986)
23. G. Evans, J. Blackledge, P. Yardley, *Numerical Methods for Partial Differential Equations*, 2nd edn. (Springer, Berlin, 2001)
24. O.C. Zienkiewicz, R.L. Taylor, *The Finite Element Method. Vol. I. Basic Formulations and Linear Problems* (McGraw-Hill, London, 1989)
25. The Mathworks, Matlab 7.4 User's Guide, http://www.mathworks.com/products/matlab/ (The Mathworks, Natick, 2007)
26. G. Milani, F. Milani, Macromol. Theory Simul. **18**, 336–354 (2009)